ISSN: 2347-467X, Vol. 13, (Special Issue) 2025, Pg. 113-123

Current Research in Nutrition and Food Science

www.foodandnutritionjournal.org

Inhibition of Calcium Oxalate Crystal Growth in Gel by Macrotyloma uniflorum, *Phaseolus lunatus*, Phaseolus vulgaris

SALMAN AHMED[1], MUHAMMAD MOHTASHEEMUL HASAN[1] ZAFAR ALAM MAHMOOD[2], JAMELAH SALEH AL-OTAIBI[3] and HAROON KHAN[4,5*]

[1]Department of Pharmacognosy, Faculty of Pharmacy and Pharmaceutical Sciences, University of Karachi, Karachi, Pakistan.
[2]Colorcon Limited – UK, Flagship House, Victory Way, Crossways, Dartford, Kent, England.
[3]Department of Chemistry, College of Science, Princess Nourah Bint Abdulrahman University, Riyadh, Kingdom of Saudi Arabia.
[4]Department of Pharmacy, Abdul Wali Khan University Mardan, Mardan, Pakistan .
[5]Department of Pharmacy, Korea University, Sejong, South Korea.

Abstract

This study investigated the inhibitory effects of aqueous seed infusions from *Macrotyloma uniflorum* (MU), *Phaseolus lunatus* (PL), and Phaseolus vulgaris (PV) on calcium oxalate monohydrate (COM) crystal growth, a key factor in kidney stone formation. Infusions at concentrations of 5%, 10%, 15%, and 20% were tested using an in vitro gel technique with phytic acid (PA) as a control. After 40 days, SEM analysis revealed irregular, incompletely formed crystals in treated samples compared to well-formed prismatic structures in controls. Morphological changes included dumbbell shapes in PA-treated and prismatic or rosette forms in MU-treated crystals. EDS analysis showed reduced calcium content and increased carbon and oxygen levels, while FTIR confirmed significant functional group modifications, especially with MU. The inhibitory effect was dose-dependent, with MU showing the strongest inhibition, followed by PV and PL, suggesting MU's potential as a natural preventive agent against calcium oxalate stone formation.

Article History
Received: 03 February 2025
Accepted: 10 April 2025

Keywords
Antiurolithiatic Activity;
Calcium Oxalate Crystals;
EDS;
FTIR;
SEM.

Abbreviations

COM	Calcium oxalate monohydrate	FTIR	Fourier Transform Infrared Spectroscopy
EDS	Energy-Dispersive X-ray Spectroscopy	MU	Macrotyloma uniflorum
		PL	Phaseolus lunatus

CONTACT Haroon Khan haroonkhan@awkum.edu.pk Department of Pharmacy, Abdul Wali Khan University Mardan, Mardan, Pakistan .

Doi: https://dx.doi.org/10.12944/CRNFSJ.13.Special-Issue-July.07

PV Phaseolus vulgaris
PA Phytic acid
SEM Scanning Electron Microscopy

Introduction

A series of basic mechanical events that lead to duct obstruction or the hardness and weakening of flexible tissues through serial aggregation and crystal development comprise crystal deposition disease (Selvaraju and Vasuki, 2014). Renal stones can be divided into two groups as papillary stones which are attached to the papillary wall and secondly the sedimentary stones which are formed in cavities with low urodynamic efficacy in which sedimentation play an important role (Grases *et al*., 1997). There are three types of calcium oxalate crystals:[1] calcium oxalate monohydrate (COM).[2] calcium oxalate dihydrate (COD) or weddellite.[3] calcium oxalate trihydrate (COT) or caoxite. The COM crystals are the major component of kidney stones and COT are formed due to bacterial indisposition of the renal tract (Fischer *et al*., 2011). Crystals of calcium oxalate range in size from microns to several centimeters. Hillock growth is the process by which the stacks of small COM crystals appear as growth layers in the shape of a hill. Due to their size, these stones connected to the ends of the renal papilla can hinder the ureter's ability to flow urine when they separate. Large cationic particles with more calcium ions than COD on their surface are known as COM crystals. Because of their greater affinity for the anionic molecules found in the membranes of renal epithelial cells, these ions adhere to renal epithelial cells and form stable aggregates rather than excreting them, which results in the retention of minerals in the renal collecting ducts for urolithiasis (Wesson and Ward, 2007). COD can crystallize preferentially over COM due to urinary inhibitors of crystal formation. These COD crystals are frequently expelled during urination and are present in healthy individuals and stone formers' urine (Chien *et al*., 2009). Since COD is frequently expelled during urination and is very weakly adherent to renal epithelial cells rather than being retained as urolith, it can be said that in vivo COD production guards against urolithiasis (Wesson and Ward, 2007, Chien *et al*., 2009).

Medicinal plants have been used for centuries due to their safety, efficacy, cultural acceptability and better safety profile as compared to modern medicine. In a study of 503 antiurolithiatic plants of 119 families and 365 genera used in different countries and cultures of the world with reported pharmacological activities, Asteraceae (41species); Fabaceae (34 species) and Lamiaceae (26 species) were most dominant families with respect to antiurolithiatic activity(Ahmed *et al*., 2016a, Kain *et al*., 2018).

Macrotyloma uniflorum (Lam) Verdc. (MU), a member of the Fabaceae family, referencing the knobby sutures on its pods. Ethnopharmacologically, in India and Pakistan, its seeds treat asthma, bronchitis, colic, diarrhoea, dysuria, hepatomegaly, hiccup, kidney stones, leucorrhea, obesity, and splenomegaly. Phytochemically, it contains anthocyanins, flavonoids, phenolic acids, tannins, and phytic acid (PA). Pharmacologically, extracts of MU have shown multiple activities, including antihypercholesterolemic, antimicrobial, antidiabetic, analgesic, anti-inflammatory, antihistaminic, anticholelithiatic, anti-peptic ulcer, anthelmintic, antioxidant, antiobesity, diuretic, hepatoprotective, larvicidal, proteinase inhibition, and nephroprotective effects (Kaundal *et al*., 2019, Patel and Niyati, 2020, Oli *et al*., 2024).

Phaseolus lunatus L. (PL) commonly known as Lima bean or Butter bean belongs to the Fabaceae family. Ethnopharmacologically, the seeds are used in India and Pakistan to treat fever, while in Africa, powdered seeds are applied to minor wounds and abscesses to promote healing. Nutritionally, PL seeds are rich in carbohydrates, proteins, and lipids and contain essential vitamins and minerals such as calcium, magnesium, phosphorus, potassium, sodium, iron, and zinc. Phytochemical analysis reveals the presence of compounds like coumestrol, kievitol, cyanogenic glycosides, and lectins. Pharmacologically, extracts of PL exhibit antidiabetic, antifungal, antiproliferative, hypocholesterolemic, and enzyme inhibition activities (Saleem *et al*., 2016a, Adebo, 2023).

Phaseolus vulgaris L. (PV) known as Kidney bean, Snap bean, Green bean belongs to the Fabaceae family. Ethnopharmacologically, the seeds are known for their diuretic properties and are used to treat kidney and heart ailments and mild diarrhea. Nutritionally, PV seeds are rich in carbohydrates, proteins, lipids, and essential vitamins and minerals, including calcium, magnesium, phosphorus, potassium, and sodium. Phytochemical studies reveal the presence

of anthocyanins, brassinosteroids, various phenolic acids, coumestrol, daidzein, +genistein, kaempferol, quercetin, and more. Pharmacologically, extracts of PV exhibit analgesic, antiobesity, antibacterial, anticancer, anti-inflammatory, hepatoprotective, antidiabetic, antioxidant, hypolipidemic, litholytic, and enzyme-inhibitory activities (Saleem *et al*., 2016b, Bhide *et al*., 2022).

This study explored the inhibitory effects of aqueous seed infusions derived from MU, PL and PV on the growth of calcium oxalate monohydrate (COM) crystals, a key contributor to kidney stone formation.

Experimental Design

Plant Specimens, Authentication, and Preparation

MU, PL, and PV seeds were purchased from a local market in Karachi. A taxonomist (Dr. Shaukat Ali) from the University of Karachi's Department of Botany identified the seeds. MU (G.H.No.86483), PL (G.H.No.86451), and PV (G.H.No.86536) all had their voucher specimen numbers assigned and placed in the University of Karachi's herbarium. The seeds were ground into a fine powder separately, sieved through a 600 µm screen, and stored at room temperature in an amber bottle.

Com Crystals Growth I In Gel

Whewellite crystals were grown by using previously described protocols (Joshi *et al*., 2005).

Preparation of Infusions

For the preparation of infusions, the seed powder (25 g) of each was separately soaked in 100 ml DDW for 24 h then the mixtures were filtered with Whatman general-purpose filter paper followed by Whatman grade No.2 filter paper thrice to get clear filtrate. As a result, dark brown colored filtrate of MU, light brown of PL, and milky infusion of PV were obtained. From these three 25 % infusions, the dilutions of 20, 15, 10, and 5 % were prepared for the study.

Pa Solution Preparation

A 5% PA stock solution was made in DDW. Using a stock solution and the serial dilution approach, reference solutions of 4, 3, 2, and 1% were created.

Com Crystal Growth

Crystal growth methods earlier reported for COM(Joshi *et al*., 2005) were adopted. All these experiments were carried out at room temperature (25 ± 2 °C). Gel media (20 ml) specified for each type of crystal was transferred to respective tubes. After gel formation, the seedling (supernatant) solution was gently poured along the wall of the test tube dropwise without disturbing the gel, then the test tubes were capped tightly. Seedling solutions were poured at the upper side of the settled gel in the left limb of U-tube and for control, standard and test solutions (20 ml) were added as given below.

Control solution: 10 ml, 1 M calcium chloride + 10 ml, 1 M magnesium acetate.

Standard solution: 5 ml, 1 M calcium chloride + 5 ml, 1 M magnesium acetate + 10 ml of 1, 2, 3, 4, 5 % PA solution respectively.

Test solutions: 5 ml, 1 M calcium chloride + 5 ml, 1 M magnesium acetate + 10 ml of 5, 10, 15, 20, 25 % tested plant infusion respectively.

Recovery of Harvested Crystals

After growth completion of COM (40 days), the gel in the test tubes was separated, removed and dispersed into DDW in a petri dish. The harvested (grown) crystals were carefully recovered from gel. These crystals were washed three times with DDW and dried with blotting paper. All the dried crystals obtained from the same test tube were weighed collectively to obtain mean weight of harvested crystals. After each experiment the U-tubes and test tubes were washed with distilled water (thrice) followed by washing with 5 % formic acid solution and finally with DDW so as to remove any contaminants from the tubes. The dried crystals were kept separately in a washed and dried glass vial for characterization through SEM, EDS and FTIR.

Characterization of Harvested Crystals

SEM

The crystals were subjected to high-resolution surface imaging by scanning electron microscopy. For SEM, JSM-6380A scanning electron microscope (JEOL, Japan) with highly vacuumed space for sample and accelerating voltage of 20 kV was used. Samples were loaded in SEM and analyzed directly (Kesavan *et al*., 2012).

EDS

The EDS measurements were carried out by an EDS detector for the standard and test samples at

different points on the crystal surface after taking SEM images. For EDS investigation, EX-54175 JMU energy dispersive spectrophotometer (JEOL, Japan) was used. Each EDS spectrum is expressed as the mass percentage of elements detected in standard and tested samples, based on ZAF Method Standard less Quantitative Analysis (standard specimen measurement not necessary), covering the energy range (0 - 20 keV) at 20.0 kV. ZAF is a very common algorithm, where Z indicates the atomic number of the element. A and F represent absorbance and fluorescence values to compensate for the X-ray peak interaction respectively (Kesavan *et al*., 2012).

The FTIR spectra of standard (commercially available compound), control (harvested crystals) and treated (crystals treated with different plant infusions) compounds were recorded in KBr phase using FTIR spectrophotometer at spectral range 4000 - 400 cm-1. For this purpose, IR Prestige-21 FTIR spectrophotometer (Shimadzu, Japan) was used. Samples were prepared by grinding 99 % KBr with 1 % of sample in Agate mortar and pestle to achieve fine homogenize form to prepare the disc. The same disc was carefully inserted in sample holder. Sample holder was inserted into FTIR spectrophotometer to record spectra(Valarmathi *et al*., 2010).

Analysis of Statistics

The unpaired student t-test was used to assess the crystal weights, which are represented as mean ± standard error of the mean.

Table 1: % inhibition of PA, MU, PL and PV treated COM crystals

COM			
Treatments	**Concentration (%)**	**Average crystal wt. (gm) ± S.E.M**	**Inhibition (%)**
Control (40days)	--------	0.808±0.01	--------
PA	1	0.447±0.0003**	44.67
	2	0.294±0.0008**	63.61
	3	0.205±0.0008**	74.62
	4	0.164±0.0008**	79.70
	5	0.073±0.0020**	90.96
MU	5	0.0	100
	10	0.490±0.0037*	39.35
	15	0.465 ± 0.0003**	42.45
	20	0.415±0.0003**	48.63
	25	0.269±0.003**	66.70
PL	5	0.606±0.0008**	25
	10	0.575±0.008**	28.83
	15	0.582±0.001**	27.97
	20	0.585±0.001**	27.59
	25	0.588±0.001**	27.22
PV	5	0.540± 0.004**	33.16
	10	0.544±0.0017**	32.67
	15	0.532±0.003**	34.15
	20	0.522±0.001**	35.39
	25	0.527±0.001**	34.77

Each value is a mean of three different determination ± S.E.M. *p<0.1; **p<0.01 vs. control showing significant and more significant values using unpaired Student's t-test.

Result

Crystal Growth in Gel

The study examined the effects of MU, PL, and PV infusions on COM crystal growth. In the control, white precipitates formed in U-tubes, while the standard solution turned milky white with a pungent odor. MU, PL, and PV infusions resulted in brown supernatants with no odor. Growth inhibition was strongest with 5% PA (90.96%), followed by lower PA concentrations. MU showed complete inhibition at 5%, with decreasing effects at lower concentrations. PL had the highest inhibition at 10% (28.83%), while PV was most effective at 20% (35.39%). The results are detailed in Table-1 and Photograph-1.

Characterization of Harvested Crystals

SEM

SEM studies revealed morphological changes in COM crystals due to MU, PL, and PV infusions. Control samples showed prismatic, rosette, and tetragonal bipyramidal shapes. PA treatment resulted in dumbbell, rosette, and bipyramidal crystals. MU (15–25%) formed rough prismatic crystals, while 10% MU produced smooth aggregates. PL (5, 20, 25%) caused rough prismatic crystals, whereas 10–15% PL led to rough dumbbell shapes. PV (5–10%) induced rough prismatic forms, while 15–25% PV produced rough bow-shaped crystals (Figure-1).

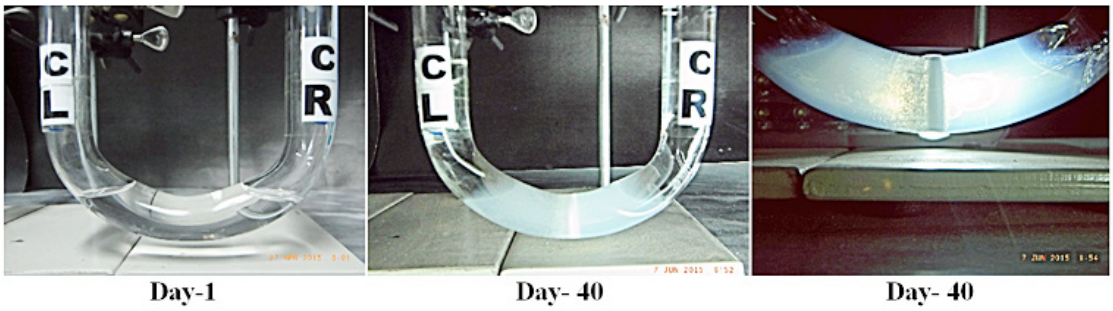

Photograph.1: COM crystals grown in gel medium after day 1 and day 40 (control).

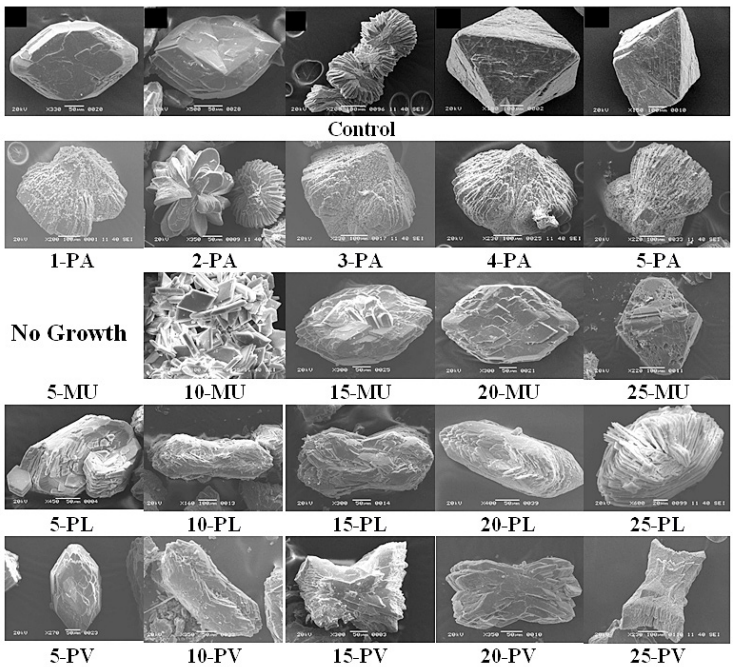

Fig.1: SEM of COM crystals. Control: prismatic, rosette, and tetragonal bipyramidal (Joshi *et al*., 2005), PA, MU, PL and PV treated COM are abnormal and deformed.

EDS

The results reveal significant variability in calcium content across samples, with extreme fluctuations in the PA, PL, and PV series, while carbon and oxygen levels remain relatively stable, though occasional outliers like high carbon in 10PL (21.19%) and low oxygen in 15MU (48.06%) are observed, suggesting differences in composition. The treatments varied in their impact on calcium retention. PA treatments, particularly 5PA (0.83%), and PL treatments, such as 10PL (0.42%), were the most inhibitory, causing the greatest calcium loss. PV treatments showed moderate inhibition, with calcium levels fluctuating from a low of 5.76% in 25PV to a peak of 27.31% in 20PV. In contrast, MU treatments retained calcium relatively well, with levels ranging from 19.13% to 23.30%, while PL treatment 20PL exhibited the highest calcium content at 33.91%, demonstrating the least inhibitory effects on calcium retention (Table – 2)

Table 2: EDS of COM

Elements (mass %)	Calcium	Carbon	Oxygen
Harvested	27.72	13.46	58.82
1PA	6.11	14.88	59.92
2PA	20.46	14.49	64.41
3PA	1.64	16.20	64.76
4PA	5.22	14.75	58.97
5PA	0.83	13.66	65.25
10MU	19.13	17.76	63.11
15MU	23.30	16.67	48.06
20MU	21.23	14.92	61.48
25MU	19.98	14.58	64.87
5PL	19.97	15.44	63.09
10PL	0.42	21.19	45.50
15PL	16.85	20.22	58.58
20PL	33.91	11.56	50.71
25PL	23.73	12.76	63.51
5PV	1.22	14.67	61.31
10PV	2.47	12.75	61.34
15PV	26.36	14.82	58.33
20PV	27.31	12.04	60.65
25PV	5.76	23.18	51.37

FTIR

The study analyzed the Fourier-transform infrared (FTIR) spectra of standard and harvested calcium oxalate monohydrate (COM) crystals, as well as those treated with various agents (PA, MU, PL, and PV). Both standard and harvested crystals exhibited characteristic absorptions for calcium oxalate, including peaks at 1622.13, 950.91, 883.40, and 781.17 cm^{-1}, confirming the presence of oxalate groups. OH stretching vibrations were observed around 3400-3500 cm^{-1}, indicating water molecules, while C=O and C-O stretching bands were identified at 1321-1373 cm^{-1} and 1089 cm^{-1}, respectively. PA-treated COM showed similar OH and C=O stretching patterns, while MU-treated COM displayed consistent OH and C=O stretches across concentrations, with an additional C-H stretch at 950.51 cm^{-1} for 20 MU. PL-treated COM exhibited OH, C=O, and C-H stretches, with variations depending on concentration. PV-treated COM also showed OH and C=O stretches, with C-H bands appearing consistently. The results are summarized in Tables 3a-3d, providing detailed FTIR values for each treatment condition.

Table-3: FTIR values of COM.

Table-3a: FTIR values of harvested and PA treated COM

Wave numbers (cm^{-1})					
COM (harvested)	**1PA-COM**	**2PA-COM**	**3PA-COM**	**4PA-COM**	**5PA-COM**
3433.29	3379.29	3402.43	3396.64	3402.43	3402.43
3061.03	-------	-------	-------	-------	-------
-------	2316.51	2335.80	2787.14, 2310.72	2328.08	2333.87
1622.13	1653	1662.64	1647.21	1647.21	1637.56
1319.31	1323.17	1371.39, 1325.10	1373.32, 1323.17	1371.39, 1325.10	1373.32, 1325.10
1089.78	-------	1105.21	-------	1124.5	1122.57
950.91	-------	-------	-------	-------	-------
883.40	829.39	831.32	831.32	829.39	831.32
781.17	-------	-------	-------	-------	-------
651.94	686.39	686.66	686.66	688.59	684.73
514.99	505.35	503.42	503.42	503.42	505.35, 418.55

Table-3b: FTIR values of harvested and MU treated COM.

Wave numbers (cm^{-1})				
COM (harvested)	**10MU-COM**	**15MU-COM**	**20MU-COM**	**25MU-COM**
3433.29	3417.86	3410.15	3415.93	3406.29
3061.03	-------	-------	-------	-------
-------	2360.87	2357.01	2372.44	2330.01
1622.13	1629.85	1649.14	1631.78	1635.64
1319.31	1373.32, 1319.31	1373.32, 1321.24	1373.32, 1321.24	1373.32, 1323.17
1089.78	1093.64	1105.21	1109.07	1124.50
950.91	-------	-------	950.91	-------
883.40	-------	829.39	829.39	831.32
781.17	781.17	779.24	779.24	779.24
651.94	661.58	671.23	665.44	673.16
514.99	507.28	507.28	509.21	505.35

Table-3c: FTIR values of harvested COM and PL treated COM

Wave numbers (cm^{-1})					
COM (harvested)	**5PL-COM**	**10PL-COM**	**15PL-COM**	**20PL-COM**	**25PL-COM**
3433.29	3421.72	3425.58	3408.22	3408.22	3414
3061.03	3061.03	3061.03	-------	-------	-------
-------	2368.59, 2299.15	2297.22	2304.94	2362.8,	2304.94

1622.13	1639.49	1656.85	1643.35	1641.42	1635.64
1319.31	1373.32, 1321.24	1319.31	1373.32, 1323.17	1321.24	1371.39, 1323.17
1089.78	1103.28	1095.57	1107.14	1103.28	1109.07
950.91	950.91	954.76	-------	952.84	948.98
883.40	883.40, 829.39	883.40	829.39	829.39	831.32
781.17	781.17	779.24	779.24	779.24	781.17
651.94	663.51	661.58	678.94	671.23	667.37
514.99	513.07	511.14	507.28	507.28	507.28, 422.41

Table-3d: FTIR values of harvested and PV treated COM.

Wave numbers (cm^{-1})					
COM (harvested)	**5PV-COM**	**10PV-COM**	**15PV-COM**	**20PV-COM**	**25PV-COM**
3433.29	3414	3412.08	3400.5	3406.29	3408.22
3061.03	-------	-------	-------	-------	-------
-------	2291.43	2374.37	2299.15	2370.51	2295.29
1622.13	1629.85	1631.78	1635.64	1637.56	1635.64
1319.31	1373.32, 1321.24	1373.32, 1321.24	1373.32, 1323.17	1373.32, 1323.17	1373.32, 1321.24
1089.78	1114.86	-------	1120.64	1112.93	1111
950.91	948.98	948.98	947.05	-------	950.91
883.40	829.39	831.32	831.32	831.32	831.32
781.17	779.24	779.24	781.17	-------	779.24
651.94	667.37	667.37	678.94	673.16	669.30
514.99	509.21	507.28	505.35	507.28	507.28

Discussion

In gel crystal growth, PA showed growth inhibition with dose dependent linear manner. MU has shown COM inhibition in following order: 5 % MU > 25 % MU > 20 % MU > 15 % MU > 10 % MU. In case of PL, inhibition was observed as 10 % PL > 15 % PL > 20 % PL > 25 % PL > 5 % PL, whereas, PV showed inhibitory effect as 20 % PV > 25 % PV > 15 % PV > 5 % PV > 10 % PV. On the basis of these results, it may be implied that MU showed most significant role in COM crystallization inhibition while PL infusion was found least active.

There is no single technique which can provide the complete information about structure and composition of urinary crystals. Microscopic features of crystals can be studied by SEM which helps in identification of micro crystalline phase. The EDS technique provides elemental composition. FTIR confirm the presence of various functional groups (Joshi *et al*., 2014). Therefore, harvested crystals were characterized by SEM, EDS and FTIR techniques.

The SEM findings highlight the structural modifications induced by different treatments, emphasizing their role in inhibiting COM crystal growth. The appearance of urinary calculi by SEM permits identification based on textural grounds (Joshi *et al*., 2014). The incompletely formed rough surface prismatic (10-25MU, 5 and 20-25 PL), dumbbell (1 and 5PA, 10 and 15 PL) and rosettes (2 PA) were observed. These disturbed and defected surfaces of COM crystals by these treatments showed antiurolithiatic effect. Tetragonal bipyramidal crystals obtained in case of 3PA and 4PA shows COD formation which is unable to participate in urolithiasis.

The EDS technique has been employed to investigate the composition of different types of urinary crystals(Joshi *et al*., 2014). PA treatments

(e.g., 5PA at 0.83%) and PL treatments (e.g., 10PL at 0.42%) were most inhibitory to calcium, PV treatments showed moderate inhibition with fluctuations (5.76–27.31%), and MU treatments, along with 20PL (33.91%), were least inhibitory, retaining the most calcium.

In the light of FTIR results in respect of mismatch it may be said that COM is most strongly affected by 1 – 5 PA and 20 PV; moderately affected by 10 MU, 15 MU, 25 MU, 15 PL, 25 PL and 5 – 15 PV. The weakly affected COM is observed in 20 MU, 20 PL and 25 PV whereas, 5 PL and 10 PL gives weakest antiurolithiatic effect response. Due to the complete inhibition of 5 MU-COM, the FTIR cannot be determined.

Phytic acid inhibits the formation of calcium oxalate monohydrate (COM) crystals by suppressing the crystallization of calcium oxalate and calcium phosphate in both renal tissues and urine (Kim *et al*., 2020). MU, PL, and PV seeds are potential prophylactic agents against urolithiasis, demonstrating their potential to prevent this condition. They leverage their diverse therapeutic properties, including analgesic, antioxidant, astringent, diuretic, and emollient effects, alongside their rich composition of phytic acid (Ahmed *et al*., 2016b).

Seeds of MU, PL and PV are reported to possess litholytic activity due to PA content which may be helpful in preventing the formation of stones. The highest level of PA (mg/g) was recorded in MU (37) followed by in PL (30.3) and in PV (33.6) (Ahmed *et al*., 2017).

Present study was taken into consideration in view of importance of antiurolithiatic phytopharmaceuticals from genus Macrotyloma and Phaseolus. Comprehensive data have been generated for MU, PL and PV which indicated the usefulness and application in the management of urolithiasis. The seeds of MU, PL and PV have been investigated extensively for macro and micro mineral contents and the key components – PA and polyphenols. The role of these macro and micro minerals along with PA and polyphenols have been correlated with antiurolithiatic effect using gel technique, an in vitro methodology reported as a suitable means to investigate phytochemicals against the development of COM urinary crystals. The overall results obtained from the present study indicated the beneficial effect of MU upon COM followed by PL, whereas least effect was observed through PV. It is believed that the data presented in the present study will be highly useful for the academic institutions and commercial manufacturers of antiurolithiatic preparations based on phytopharmaceuticals.

Limitations of the Study

Despite the promising findings, the study has several limitations. Firstly, the in vitro gel technique used for evaluating antiurolithiatic effects may not fully replicate the physiological conditions of the human urinary system. Factors such as urinary pH, ionic concentration, and presence of other urinary inhibitors or promoters may influence crystallization differently in vivo. Secondly, while SEM, EDS, and FTIR provided valuable insights into crystal morphology and composition, additional techniques such as X-ray diffraction (XRD) and Raman spectroscopy could further enhance structural characterization. Thirdly, the study did not assess the bioavailability, metabolism, and pharmacokinetics of the phytochemicals in MU, PL, and PV, which are critical for their therapeutic application. Lastly, the study lacked an in vivo validation component, which would be essential to confirm the antiurolithiatic potential of these seeds under physiological conditions. Future research should focus on in vivo studies, clinical trials, and mechanistic insights to substantiate the findings and improve the translational applicability of these phytopharmaceuticals.

Conclusion

This study investigates the antiurolithiatic potential of phytopharmaceuticals derived from Macrtyloma uniflorum, *Phaseolus lunatus*, and Phaseolus vulgaris seeds, identifying Macrtyloma uniflorum as the most effective against COM crystals, followed by *Phaseolus lunatus* and Phaseolus vulgaris. The SEM, EDS, and FTIR analyses confirmed the structural and compositional changes in the crystals, reinforcing the antiurolithiatic potential of these seeds. The high content of phytic acid in Macrtyloma uniflorum, *Phaseolus lunatus*, and Phaseolus vulgaris seeds supports their therapeutic use in preventing urolithiasis, with Macrtyloma uniflorum being the most effective. These findings suggest their potential application in phytopharmaceutical

formulations for managing kidney stones. The findings highlight the need for further ex vivo, in vivo, and XRD studies to advance clinical applications.

Acknowledgement
The authors extend their appreciation to the Princess Nourah Bint Abdulrahman University.

Funding sources
Researchers Supporting Project number (PNURSP2025R13), Princess Nourah Bint Abdulrahman University, Saudi Arabia for funding.

Conflict of interest
The authors do not have any conflict of interest.

Data Availability Statement
The data can be provided upon request.

Ethics Statement
This research did not involve human participants, animal subjects, or any material that requires ethical approval.

Informed Consent Statement
This study did not involve human participants, and therefore, informed consent was not required.

Clinical Trial Registration
This research does not involve any clinical trials.

Permission to Reproduce Material from Other Sources
Not Applicable.

Author Contributions
- **Salman Ahmed -** performed the experiments, analyzed the data and writing - original draft, writing.
- **Muhammad Mohtasheemul Hasan -** conceptualization, supervision,
- **Zafar Alam Mahmood -** conceptualization, supervision,
- **Jamelah Saleh Al-Otaibi -** review the overall manuscript, edited to its final draft. All the authors approve the final version of the article.
- **Haroon Khan -** review the overall manuscript, edited to its final draft. All the authors approve the final version of the article.

References

1. Adebo, J. A. 2023. A Review on the Potential Food Application of Lima Beans (*Phaseolus lunatus* L.), an Underutilized Crop. *Applied Sciences,* 13, 1996.
2. Ahmed, S., Hasan, M. & Mahmood, Z. 2016a. Antiurolithiatic plants: multidimensional pharmacology. *Journal of Pharmacognosy and Phytochemistry*, 5, 04-24.
3. Ahmed, S., Hasan, M. M., Mahmood, Z. A., House, F. & Way, V. 2016b. *Macrotyloma uniflorum* (Lam.) Verdc, *Phaseolus lunatus* Linn, Phaseolus vulgaris Linn. seeds: Nature's potential candidates against urolithiasis by virtue of multidimensional pharmacology. *World Journal of Pharmacy and Pharmaceutical Sciences,* 5, 289-300.
4. Ahmed, S., Mahmood, S. B. Z., Hasan, M. M. & Mahmood, Z. A. 2017. Essential minerals and phytic acid in legumes with reference to their nutritive and medicinal properties. *Pakistan Journal of Pharmaceutical Sciences,* 30, 1733-1742.
5. Bhide, Y., Nehete, J. & Bhambar, R. 2022. Botanical, chemical and pharmacological review of Phaseolus vulgaris L. (common bean): An ayurvedic medicinal plant. *International Journal of Health Sciences,* 6, 11527-11543.
6. Chien, Y.-C., Masica, D. L., Gray, J. J., Nguyen, S., Vali, H. & Mckee, M. D. 2009. Modulation of calcium oxalate dihydrate growth by selective crystal-face binding of phosphorylated osteopontin and polyaspartate peptide showing occlusion by sectoral (compositional) zoning. *Journal of Biological Chemistry*, 284, 23491-23501.
7. Fischer, V., Landfester, K. & Munoz-Espi, R. 2011. Stabilization of calcium oxalate metastable phases by oligo (L-glutamic acid): effect of peptide chain length. *Crystal Growth*

& Design, 11, 1880-1890.

8. Grases, F., Prieto, R. & Costa-Bauza, A. 1997. In vitro models for studying renal stone formation: a clear alternative. *Alternatives to laboratory animals*: ATLA, 26, 481-503.
9. Joshi, V., Parekh, B., Joshi, M. & Vaidya, A. 2005. Herbal extracts of Tribulus terrestris and Bergenia ligulata inhibit growth of calcium oxalate monohydrate crystals *in vitro. Journal of Crystal Growth,* 275, e1403-e1408.
10. Joshi, V., Vasant, S. R., Bhatt, J. & Joshi, M. J. 2014. some critical aspects of FT-IR,TGA, powder XRD, EDAX and SEM studies of calcium oxalate urinary calculi*. Indian Journal of Biochemistry and Biophysics,* 51, 237-243.
11. Kain, D., Kumar, S. & Suryavanshi, A. 2018. Therapeutic values of medicinal plants against prevalence of Urolithiasis: A Review. *Medicinal Plants-International Journal of Phytomedicines and Related Industries,* 10, 268-277.
12. Kaundal, S. P., Sharma, A., Kumar, R., Kumar, V. & Kumar, R. 2019. Exploration of medicinal importance of an underutilized legume crop, *Macrotyloma uniflorum* (Lam.) Verdc.(Horse gram): A review. *Int. J. Pharm. Sci. Res,* 10, 3178-86.
13. Kesavan, M., Kaliaperumal, R., Tamilmani, E. & Shanmugam, K. 2012. In vitro evaluation of calcium oxalate monohydrate crystals influenced by Costus igneus aqueous extract. *Scandinavian Journal of Urology and Nephrology,* 46, 290-297.
14. Kim, O.-H., Booth, C. J., Choi, H. S., Lee, J., Kang, J., Hur, J., Jung, W. J., Jung, Y.-S., Choi, H. J., Kim, H., Auh, J.-H., Kim, J.-W., Cha, J.-Y., Lee, Y. J., Lee, C. S., Choi, C., Jung, Y. J., Yang, J.-Y., Im, S.-S., Lee, D. H., Cho, S. W., Kim, Y.-B., Park, K. S., Park, Y. J. & Oh, B.-C. 2020. High-phytate/low-calcium diet is a risk factor for crystal nephropathies, renal phosphate wasting, and bone loss. eLife, 9, e52709.
15. Oli, P., Joshi, K. & Punetha, S. 2024. Traditional uses, phytochemistry, pharmacology, and nutraceutical potential of horse gram (Macrotyloma uniflorum): A systematic review. *Journal of Food Science,* 89, 8102-8127.
16. Patel, V. & Niyati, A. 2020. Anti-urolithiatic activities of *Macrotyloma uniflorum* Mediated through Multiple Pathway. *Indian Journal of Pharmaceutical Education and Research*, 54, 403-415.
17. Saleem, Z. M., Ahmed, S. & Hasan, M. M. 2016a. *Phaseolus lunatus* linn: Botany, medicinal uses, phytochemistry and pharmacology. *World Journal of Pharmacy and Pharmaceutical Sciences,* 5, 87-93.
18. Saleem, Z. M., Ahmed, S. & Hasan, M. M. 2016b. Phaseolus vulgaris linn.: botany, medicinal uses, phytochemistry and pharmacology. *World Journal of Pharmaceutical Research,* 5, 1611-1616.
19. Selvaraju, R. & Vasuki, G. 2014. Growth of calcium hydrogen phosphate dihydrate (CHPD) crystal and characterization studied by spectral method. *International Journal of Current Advanced Research*, 3, 40-42.
20. Valarmathi, D., Abraham, L. & Gunasekaran, S. 2010. Growth of calcium oxalate monohydrate crystal by gel method and its spectroscopic analysis. *Indian Journal of Pure and Applied Physics*, 48, 36-8.
21. Wesson, J. A. & Ward, M. D. 2007. Pathological biomineralization of kidney stones. *Elements,* 3, 415-421.